FIG 3 Estimated Bayesian skyride plot of the CRF01_1b2k clade. The vertical axis represents the product of viral generation time and the effective number of infections (N_e). The solid line shows the best estimate, and the shaded area shows the 95% credible region of this estimate.

restricting the opportunities for HCV to generate CRFs. Mixed infections with divergent HCV strains have been reported for many different populations and are noted to be prevalent among high-risk groups, particularly IDUs and some hemophiliacs (3, 5, 16, 50, 53).

Since the opportunities for HCV recombination are not limited, it is more likely that fundamental molecular and evolutionary differences between HIV and HCV explain why HIV has many CRFs and HCV has few. These could include differences in the rate of template switching or differences in genomic or immunological constraints, such that HCV recombinants have, on average, lower fitness than HIV recombinants and therefore are rarely transmitted (72). Although both viruses are associated with chronic infections, unlike HIV, HCV can be spontaneously cleared by the host. This may explain in part the differences in the number of recombinants between HIV and HCV, where partial protective immunity against the latter reduces that chance of *in vivo* recombination of HCV strains (1, 43, 69). However, the high rate of mixed infections observed suggests that this is likely at best to play a minor role in HCV recombination. The low frequency of HCV recombinants is more likely to reflect mechanistic constraints on viral replication. There is evidence that template switching in HCV is
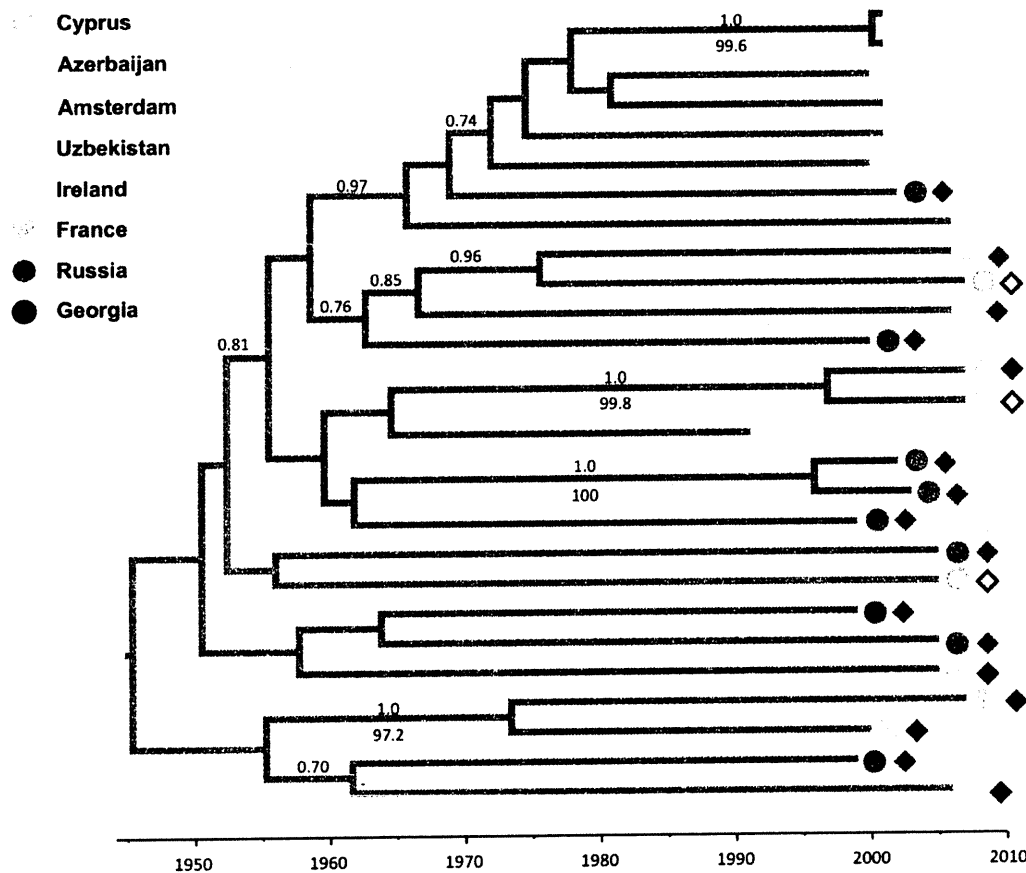
FIG 4 Molecular clock phylogeny of the CRF01_1b2k clade, estimated using a relaxed uncorrelated lognormal clock model and the SDR06 nucleotide substitution model (see Materials and Methods). Sequences are color labeled according to the country of origin (diamonds) and the country of sampling (circles). All isolates were found to have an epidemiological link to Russia or the former Soviet Union (Table 1). Filled circles/diamonds, 2k/1b isolates that were confirmed as being recombinant by sequencing of the breakpoint in the NS2 region; open circles/diamonds, those isolates for which NS2 sequences were not available. The numbers above the branches show the posterior probability of nodes in the MCC tree; numbers below the branches represent bootstrap support values using maximum likelihood.

especially rare and that the replication complex is typically encoded on the same genomic strand that it will replicate and transcribe (2). It is also interesting that when replication complexes are exchanged between different genotypes, the replication efficiency is substantially reduced (15). The pseudodiploidy of the HIV genome certainly increases the likelihood of recombination occurring due to the ability of the virus to package two RNA templates (17), while the secondary RNA structure in the HCV genome may limit the production of viable hybrid HCVs (59, 68).

Our study of previously reported and newly obtained HCV isolates provides the first estimates of the date of the recombination event that generated CRF01_1b2k. We estimated the time of origin of CRF01_1b2k to be between 1923 and 1956, which is not much later than the origin and global spread of the parental subtype 1b (33). This date is significantly earlier than we expected: we expected that the CRF's creation might be linked to the dramatic increase in IDU behavior following the breakup of the former Soviet Union. This result is robust to the manner of isolate sampling: if, because of nonrandom sampling, our isolates are more closely related to each other than under random sampling, then the TMRCA of CRF01_1b2k would be biased toward more recent dates. Furthermore, despite its small size, our data set provides a relatively short time window during which the recombinant must have arisen (Fig. 2). The involvement of subtype 1b in the recombinant is not surprising, as it is one of the most prevalent subtypes worldwide. However, to fully appreciate the origin of CRF01_1b2k, we need to consider the evolutionary history of both parental subtypes and of the recombinant lineage itself. Genotype 2 harbors considerable genetic diversity, especially in West Africa, which is where the genotype is thought to have originated (34). Although the small number of subtype 2k isolates sampled to date likely underestimates the true extent of subtype 2k distribution, such viruses have been isolated from Martinique and Madagascar, implicating a role for the historical trans-Atlantic slave trade in the dissemination of the virus from West Africa (34).

The current distribution of subtype 2k is associated with francophone regions and former Soviet Union countries. In contrast, CRF01_1b2k is more spatially limited, with all isolates being directly or indirectly linked to the former Soviet Union. As the non-recombinant subtype 2k isolates that are most closely related to CRF01_1b2k are from Moldova and Azerbaijan (see Fig. S1 in the supplemental material), it seems most likely that CRF01_1b2k was generated in the former Soviet Union. An equivalent analysis of subtype 1b viruses provides no reliable phylogeographic linkage, due to the low phylogenetic resolution of the NS5B data set.

Our estimated date of CRF origin coincides with an interesting period of history in the former Soviet Union, which was an early leader in transfusion technology. Under the leadership of Alexander Bogdanov in the 1920s, a nationwide network of blood transfusion centers and research institutes, as well as the Central Institute of Hematology in Moscow, Russia, in 1926, was established throughout the Soviet republics (61). This expanded into a network of ~1,500 blood donating centers across the republics (18). The Soviets also adopted blood storage and preservation techniques at an early stage. They established more than 60 primary and 500 subsidiary blood storage centers by the mid-1930s, which shipped blood across the entire Soviet Union (61). During the Second World War, these networks were swiftly readapted to support the front line; in Moscow alone, about 2,000 blood donations were given per day (18, 61). The impressive scale of the blood

service in the former Soviet Union is likely to have favored HCV transmission by increasing the efficiency and geographic range of the virus's dissemination. Whether specific medical practices at this time increased the probability of mixed viral infections remains unknown. It is interesting to note that Bogdanov himself was fascinated by the ideological interpretation of blood sharing and frequently practiced what he called "physiological collectivism": the exchange of blood with others through mutual transfusions (61).

Although unscreened blood transfusions can provide a credible hypothesis for the origin of CRF01_1b2k in the Soviet Union some time from 1923 to 1956, we must also attempt to explain how subtype 2k or the CRF itself arrived in the Soviet Union from West Africa or the Caribbean. Migration from Africa to the former Soviet Union did occur during the late 1950s and 1970s as a result of alliances forged by the Soviet government with newly independent African states such as Ghana and Angola (35). However, these connections are too late to have contributed to the emergence of CRF01_1b2k, according to our dating estimates. Although we cannot reject the hypothesis that the CRF was formed in West Africa and subsequently moved to the Soviet Union, our results are more consistent with the recombination event occurring in the latter. This uncertainty is likely to be reduced with further samples, especially subtype 2k viruses, from African and former Soviet Union locations.

The epidemic history CRF01_1b2k (Fig. 3) since its emergence is similar to that estimated for other epidemic subtypes of HCV (e.g., see reference 33). The growth in the CRF01_1b2k effective population sizes coincides with a substantial increase in blood transfusion, including during the Second World War, and with the subsequent rise in intravenous drug usage. CRF01_1b2k transmission seems to have slowed or stabilized since the early 1990s, coinciding with the onset of the anti-HCV screening of donors. In the absence of any data to the contrary, the transmission of this recombinant and its spread from the former Soviet Union reflect the peculiar epidemiological properties of the risk groups that it has been associated with rather than any intrinsic properties of the virus.

We demonstrate the practicality and benefits of using a hierarchical phylogenetic model to jointly estimate parameters of interest when analyzing multipartite sequence data that result from genetic exchange. This method yields more accurate parameter estimates than previous methods (e.g., see references 27 and 67) by incorporating the phylogenetic information and uncertainty in different genomic regions. We recommend that this improved statistical framework be used in future investigations of recombination in fast-evolving RNA viruses.

This study has made significant steps in understanding the epidemic history and spread of the unique circulating HCV recombinant 2k/1b. Most significantly, we show that this strain originated many decades before the post-Soviet rise in injection behavior with which it is currently associated. On the basis of the date of its origin and its molecular epidemiology, there are reasonable grounds to suppose that the Soviet Union's revolutionary blood service was instrumental in the CRF's early generation and continental-scale spread. This infrastructure may have facilitated the pan-Eurasian spread of other parenterally transmitted bloodborne infections, and this is an interesting question for future research.

REFERENCES

1. Aitken CK, et al. 2008. High incidence of hepatitis C virus reinfection in a cohort of injecting drug users. Hepatology 48:1746–1752.
2. Appel N, Herian U, Bartenschlager R. 2005. Efficient rescue of hepatitis C virus RNA replication by trans-complementation with nonstructural protein 5A. J. Virol. 79:896–909.
3. Blackard JT, Sherman KE. 2007. Hepatitis C virus coinfection and superinfection. J. Infect. Dis. 195:519–524.
4. Boom R, et al. 1990. Rapid and simple method for purification of nucleic-acids. J. Clin. Microbiol. 28:495–503.
5. Bowden S, McCaw R, White PA, Crofts N, Aitken CK. 2005. Detection of multiple hepatitis C virus genotypes in a cohort of injecting drug users. J. Viral Hepat. 12:322–324.
6. Calado RA, et al. 2011. Hepatitis C virus subtypes circulating among intravenous drug users in Lisbon, Portugal. J. Med. Virol. 83:608–615.
7. Colina R, et al. 2004. Evidence of intratypic recombination in natural populations of hepatitis C virus. J. Gen. Virol. 85:31–37.
8. Cristina J, Colina R. 2006. Evidence of structural genomic region recombination in hepatitis C virus. Virology J. 3:53.
9. Demetriou VL, de Vijver DAMCV, Kostrikis LG, Network CHCV. 2009. Molecular epidemiology of hepatitis C infection in Cyprus: evidence of polyphyletic infection. J. Med. Virol. 81:238–248.
10. Drummond AJ, Ho SYW, Phillips MJ, Rambaut A. 2006. Relaxed phylogenetics and dating with confidence. PLoS Biol. 4:699–710.
11. Drummond AJ, Rambaut A. 2007. BEAST: Bayesian evolutionary analysis by sampling trees. BMC Evol. Biol. 7:214.
12. Drummond AJ, Rambaut A, Shapiro B, Pybus OG. 2005. Bayesian coalescent inference of past population dynamics from molecular sequences. Mol. Biol. Evol. 22:1185–1192.
13. Dubois F, et al. 1997. Hepatitis C in a French population-based survey, 1994: seroprevalence, frequency of viremia, genotype distribution, and risk factors. Hepatology 25:1490–1496.
14. Gray RR, et al. 2011. The mode and tempo of hepatitis C virus evolution within and among hosts. BMC Evol. Biol. 11:131.
15. Herlihy KJ, et al. 2008. Development of intergenotypic chimeric replicons to determine the broad-spectrum antiviral activities of hepatitis C virus polymerase inhibitors. Antimicrob. Agents Chemother. 52:3523–3531.
16. Herring BL, Page-Shafer K, Tobler LH, Delwart EL. 2004. Frequent hepatitis C virus superinfection in injection drug users. J. Infect. Dis. 190:1396–1403.
17. Hu WS, Temin HM. 1990. Genetic consequences of packaging two RNA genomes in one retroviral particle: pseudodiploidy and high rate of genetic recombination. Proc. Natl. Acad. Sci. U. S. A. 87:1556–1560.
18. Huestis DW. 2002. Russia's National Research Center for Hematology: its role in the development of blood banking. Transfusion 42:490–494.
19. Kageyama S, et al. 2006. A natural inter-genotypic (2b/1b) recombinant of hepatitis C virus in the Philippines. J. Med. Virol. 78:1423–1428.
20. Kalinina O, Norder H, Mukomolov S, Magnius LO. 2002. A natural intergenotypic recombinant of hepatitis C virus identified in St. Petersburg. J. Virol. 76:4034–4043.
21. Kalinina O, et al. 2001. Shift in predominating subtype of HCV from 1b to 3a in St. Petersburg mediated by increase in injecting drug use. J. Med. Virol. 65:517–524.
22. Kapoor A, et al. 2011. Characterization of a canine homolog of hepatitis C virus. Proc. Natl. Acad. Sci. U. S. A. 108:11608–11613.
23. Kuiken C, Simmonds P. 2009. Nomenclature and numbering of the hepatitis C virus. Methods Mol. Biol. 510:33–53.
24. Kuiken C, Yusim K, Boykin L, Richardson R. 2005. The Los Alamos hepatitis C sequence database. Bioinformatics 21:379–384.
25. Kurbanov F, et al. 2008. Detection of hepatitis C virus natural recombinant RF1_2k/1b strain among intravenous drug users in Uzbekistan. Hepatol. Res. 38:457–464.
26. Kurbanov F, et al. 2008. Molecular epidemiology and interferon susceptibility of the natural recombinant hepatitis C virus strain RF1_2k/1b. J. Infect. Dis. 198:1448–1456.
27. Lam TY, et al. 2008. Evolutionary analyses of European H1N2 swine influenza A virus by placing timestamps on the multiple reassortment events. Virus Res. 131:271–278.
28. Lee YM, et al. 2010. Molecular epidemiology of HCV genotypes among injection drug users in Taiwan: full-length sequences of two new subtype 6w strains and a recombinant form_2b6w. J. Med. Virol. 82:57–68.
29. Legrand-Abravanel F, et al. 2007. New natural intergenotypic (2/5) recombinant of hepatitis C virus. J. Virol. 81:4357–4362.
30. Leitner T, Korber B, Daniels M, Calef C, Foley B. 2005. HIV-1 subtype and circulating recombinant form (CRF) reference sequences, 2005, p 41–48. In Leitner T, et al (ed), HIV sequence compendium 2005. Theoretical Biology and Biophysics Group, Los Alamos National Laboratory, Los Alamos, NM.
31. Lemon SM, Brown EA. 1995. Hepatitis C virus, p 1474–1486. In Mandel GL, Bennett JE, Dolin R (ed), Principle and practice of infectious disease, 4th ed. Churchill Livingstone, New York, NY.
32. Li Y, et al. 2010. Identification of a novel second-generation circulating recombinant form (CRF48_01B) in Malaysia: a descendant of the previously identified CRF33_01B. J. Acquir. Immune Defic. Syndr. 54:129–136.
33. Magiorkinis G, et al. 2009. The global spread of hepatitis C virus 1a and 1b: a phylodynamic and phylogeographic analysis. PLoS Med. 6:e1000198.
34. Markov PV, et al. 2009. Phylogeography and molecular epidemiology of hepatitis C virus genotype 2 in Africa. J. Gen. Virol. 90:2086–2096.
35. Matusevich M. 2009. Black in the U.S.S.R.: Africans, African Americans, and the Soviet society. Transition 100:56–75.
36. Minin VN, Bloomquist EW, Suchard MA. 2008. Smooth skyride through a rough skyline: Bayesian coalescent-based inference of population dynamics. Mol. Biol. Evol. 25:1459–1471.
37. Moreau I, et al. 2006. Serendipitous identification of natural intergenotypic recombinants of hepatitis C in Ireland. Virol. J. 3:95–102.
38. Morel V, et al. 2010. Emergence of a genomic variant of the recombinant 2k/1b strain during a mixed hepatitis C infection: a case report. J. Clin. Virol. 47:382–386.
39. Moreno P, et al. 2009. Evidence of recombination in hepatitis C virus populations infecting a hemophiliac patient. Virol. J. 6:203.
40. Murphy DG, et al. 2007. Use of sequence analysis of the NS5B region for routine genotyping of hepatitis C virus with reference to C/E1 and 5′ untranslated region sequences. J. Clin. Microbiol. 45:1102–1112.
41. Newton MA, Raftery AE. 1994. Approximate Bayesian-inference with the weighted likelihood bootstrap. J. R. Stat. Soc. Ser. B Methodol. 56:3–48.
42. Noppornpanth S, et al. 2006. Identification of a naturally occurring recombinant genotype 2/6 hepatitis C virus. J. Virol. 80:7569–7577.
43. Osburn WO, et al. 2010. Spontaneous control of primary hepatitis C virus infection and immunity against persistent reinfection. Gastroenterology 138:315–324.
44. Pawlotsky JM, et al. 1995. Relationship between hepatitis-C virus genotypes and sources of infection in patients with chronic hepatitis-C. J. Infect. Dis. 171:1607–1610.
45. Pol S, et al. 1995. The changing relative prevalence of hepatitis-C virus genotypes—evidence in hemodialyzed patients and kidney recipients. Gastroenterology 108:581–583.
46. Pybus OG, et al. 2001. The epidemic behavior of the hepatitis C virus. Science 292:2323–2325.
47. Pybus OG, Cochrane A, Holmes EC, Simmonds P. 2005. The hepatitis C virus epidemic among injecting drug users. Infect. Genet. Evol. 5:131–139.
48. Pybus OG, Drummond AJ, Nakano T, Robertson BH, Rambaut A. 2003. The epidemiology and iatrogenic transmission of hepatitis C virus in Egypt: a Bayesian coalescent approach. Mol. Biol. Evol. 20:381–387.
49. Pybus OG, Markov PV, Wu A, Tatem AJ. 2007. Investigating the endemic transmission of the hepatitis C virus. Int. J. Parasitol. 37:839–849.
50. Qian KP, Natov SN, Pereira BJ, Lau JY. 2000. Hepatitis C virus mixed genotype infection in patients on haemodialysis. J. Viral Hepat. 7:153–160.
51. Ristic N, et al. 2011. Analysis of the origin and evolutionary history of HIV-1 CRF28_BF and CRF29_BF reveals a decreasing prevalence in the AIDS epidemic of Brazil. PLoS One 6:e17485.
52. Schreiber GB, Busch MP, Kleinman SH, Korelitz JJ. 1996. The risk of transfusion-transmitted viral infections. The Retrovirus Epidemiology Donor Study. N. Engl. J. Med. 334:1685–1690.
53. Schroter M, Feucht HH, Zollner B, Schafer P, Laufs R. 2003. Multiple infections with different HCV genotypes: prevalence and clinical impact. J. Clin. Virol. 27:200–204.
54. Seeff LB, et al. 2000. 45-year follow-up of hepatitis C virus infection in healthy young adults. Ann. Intern. Med. 132:105–111.
55. Shapiro B, Rambaut A, Drummond AJ. 2006. Choosing appropriate substitution models for the phylogenetic analysis of protein-coding sequences. Mol. Biol. Evol. 23:7–9.

– 143 –

56. Shepard CW, Finelli L, Alter MJ. 2005. Global epidemiology of hepatitis C virus infection. Lancet Infect. Dis. 5:558–567.

57. Silini E, et al. 1995. Molecular epidemiology of hepatitis-C virus-infection among intravenous-drug-users. J. Hepatol. 22:691–695.

58. Simmonds P. 2004. Genetic diversity and evolution of hepatitis C virus—15 years on. J. Gen. Virol. 85:3173–3188.

59. Simmonds P, Smith DB. 1999. Structural constraints on RNA virus evolution. J. Virol. 73:5787–5794.

60. Smith DB, et al. 1997. The origin of hepatitis C virus genotypes. J. Gen. Virol. 78(Pt 2):321–328.

61. Starr D. 1999. Blood: an epic history of medicine and commerce.Little, Brown & Company, London, United Kingdom.

62. Suchard MA, Kitchen CMR, Sinsheimer JS, Weiss RE. 2003. Hierarchical phylogenetic models for analyzing multipartite sequence data. Syst. Biol. 52:649–664.

63. Suchard MA, Weiss RE, Sinsheimer JS. 2001. Bayesian selection of continuous-time Markov chain evolutionary models. Mol. Biol. Evol. 18:1001–1013.

64. Swofford D. 2003. PAUP*. Phylogenetic analysis using parsimony (*and other methods), version 4.Sinauer Associates, Sunderland, MA.

65. Tanaka Y, et al. 2004. Exponential spread of hepatitis C virus genotype 4a in Egypt. J. Mol. Evol. 58:191–195.

66. Tanaka Y, et al. 2005. Molecular evolutionary analyses implicate injection treatment for schistosomiasis in the initial hepatitis C epidemics in Japan. J. Hepatol. 42:47–53.

67. Tee KK, et al. 2009. Estimating the date of origin of an HIV-1 circulating recombinant form. Virology 387:229–234.

68. Tuplin A, Wood J, Evans DJ, Patel AH, Simmonds P. 2002. Thermodynamic and phylogenetic prediction of RNA secondary structures in the coding region of hepatitis C virus. RNA 8:824–841.

69. van de Laar TJ, et al. 2009. Frequent HCV reinfection and superinfection in a cohort of injecting drug users in Amsterdam. J. Hepatol. 51:667–674.

70. van der Poel CL. 1999. Hepatitis C virus and blood transfusion: past and present risks. J. Hepatology 31(Suppl 1):101–106.

71. WHO. 2003, posting date. Global alert and response (GAR): hepatitis C. WHO, Geneva, Switzerland.

72. Worobey M, Holmes EC. 1999. Evolutionary aspects of recombination in RNA viruses. J. Gen. Virol. 80:2535–2543.

— 144 —
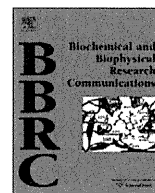
Liver tumor formation by a mutant retinoblastoma protein in the transgenic mice is caused by an upregulation of c-Myc target genes

Bo Wang [a], Keisuke Hikosaka [a], Nishat Sultana [a], Mohammad Tofael Kabir Sharkar [a], Hidenao Noritake [a,b], Wataru Kimura [a], Yi-Xin Wu [a], Yoshimasa Kobayashi [b], Tadayoshi Uezato [a], Naoyuki Miura [a,*]

[a] Department of Biochemistry, Hamamatsu University School of Medicine, 1-20-1 Handa-yama, Higashi-ku, Hamamatsu 431-3192, Japan
[b] Department of Internal Medicine, Hamamatsu University School of Medicine, 1-20-1 Handa-yama, Higashi-ku, Hamamatsu 431-3192, Japan

ABSTRACT

The retinoblastoma (Rb) tumor suppressor encodes a nuclear phosphoprotein that regulates cellular proliferation, apoptosis and differentiation. In order to adapt itself to these biological functions, Rb is subjected to modification cycle, phosphorylation and dephosphorylation. To directly determine the effect of phosphorylation-resistant Rb on liver development and function, we generated transgenic mice expressing phosphorylation-resistant human mutant Rb (mt-Rb) under the control of the rat hepatocyte nuclear factor-1 gene promoter/enhancer. Expression of mt-Rb in the liver resulted in macroscopic neoplastic nodules (adenomas) with ~50% incidence within 15 months old. Interestingly, quantitative reverse transcriptase-PCR analysis showed that c-Myc was up-regulated in the liver of mt-Rb transgenic mice irrespective of having tumor tissues or no tumor. In tumor tissues, several c-Myc target genes, Foxm1, c-Jun, c-Fos, Bmi1 and Skp2, were also up-regulated dramatically. We determined whether mt-Rb activated the Myc promoter in the HTP9 cells and demonstrated that mt-Rb acted as an inhibitor of wild-type Rb-induced repression on the Myc promoter. Our results suggest that continued upregulation of c-Myc target genes promotes the liver tumor formation after about 1 year of age.

© 2011 Elsevier Inc. All rights reserved.

1. Introduction

Human hepatocellular carcinoma (HCC) is one of the most common types of malignant cancer in Asia and Africa. HCC normally develops as a consequence of underlying liver disease and is most often associated with cirrhosis. Surgical resection and liver transplantation are current best curative options to treat liver cancer. However, recurrence or metastasis is quite common in patients who have had a resection and survival rate is 30% to 40% at 5 years postoperatively [1–4]. Although the major viral and environmental risk factors for HCC development have been unraveled, the molecular mechanism involved in hepatic carcinogenesis is still poorly understood [5].

The retinoblastoma gene is the first-identified human tumor suppressor gene and is considered as a core element governing cell cycle progression, cell proliferation, differentiation, apoptosis, and senescence through its ability to bind the transcription factor E2F-1 that activate transcription of genes required for S phase [6]. Molecular genetic studies have identified abnormalities of this tumor suppressor gene in a large proportion of human cancers including HCC [7]. Germ line mutations in the Rb gene predispose individuals to bilateral retinoblastoma as well as osteosarcoma [8,9]. Somatic Rb inactivation contributes to the development of these tumors as well as to other tumors in different organs like bladder, lung, breast and prostate [10–13].

Although a vast amount of data has been accumulated on the role of Rb in cancer development for several cancer entities, only limited insight is available on the role of Rb in HCC development [14]. Most of the data show that deregulation, loss or inactivation of Rb is an obligatory step in tumor formation. Intriguingly, studies in human HCCs showed not only absent but also a high incidence of Rb protein over-expression (~50%) [15]. This finding suggests that active Rb protein may have some interesting biological consequences that contribute to liver tumorigenesis. Now, there are two ways to investigate the function of a gene in vivo. One is to create knockout mice lacking a gene function and the other is to create transgenic mice in which the gene is expressed ectopically or over-expressed [16]. The liver-specific Rb loss in mice shows ectopic cell cycle entry and aberrant ploidy whereas the loss of Rb does not lead to any detectable hyperplasia or tumorigenesis in the liver of adult mice [17]. We found that hepatocytes in the WT-Rb transgenic mice show

resistance to fulminant hepatitis and carcinogenesis whereas its liver develops normally [16]. The over-expressed WT-Rb protein in hepatocytes can be phosphorylated, so the liver of transgenic mice does not show any chronic damages. And liver is a special organ that exhibits an exquisitely controlled cell cycle, wherein hepatocytes are maintained in quiescence until stimulated to proliferation. Previous studies showed that the phosphorylation-resistant Rb exhibits greater activity than the WT protein [18]. On these bases, we generated transgenic mice expressing phosphorylation-resistant human Rb (mt-Rb) under the control of the hepatocyte nuclear factor-1 (HNF-1) gene promoter/enhancer to predict the expression of mt-Rb protein only in the liver, not in other organ. We found that mt-Rb resulted in the c-Myc up-regulation in the liver of mt-Rb transgenic mice and then c-Myc activated several target genes in the tumor. These results indicate that up-regulation of Foxm1, Bmi1 and several target genes promotes the liver tumor formation.

2. Materials and methods

2.1. Construction of the mutant Rb transgenic mice

The animal procedures were approved by the experimental animal ethics committee at Hamamatsu University School of Medicine.

The BamHI fragment of wild-type human Rb cDNA was subcloned into pKF18 k vector (Takara, Kyoto, Japan). Site-directed mutagenesis was performed using Mutan-Express km Enzyme/Oligo Set (Takara #6090, Kyoto). Mutagenic oligonucleotides were 5'-ATGCCGCCCAAAGCCCCCCGAAAAAC-3' (T5A), 5'-GGTTCACCTCGA GCCCC CAGGCGAGGT-3' (T252A), 5'-TTTGAAACACAGAGAGCCCCAC GAAAAAGTAA C-3' (T356A), 5'-ATTCCTCCACACGCTCCAGTTAGGAC-3' (T373A), 5'-GCAGATATGTATCTTGCTCCTGTAAGAGCTCCAAAGAA AAAAGG-3' (S608A, S612A), 5'-CACATTCCTCGAGCCCCTTACAAGT TT-3' (S788A), 5'-CCTTACAAGTTTCCTAGTGCCCCCTTACGGATTCC-3' (S795A), 5'-GGGAACATCTATATTGCCCCCCTGAAGGCTCCATATAAA-ATTTCAGAA-3' (S807A, S811A), 5'-GAAGGTCTGCCAGCCCCAACA AAAATGACT-3' (T821A) and 5'-ATACCCATTAATGGTGCACCTCGAGC CC-3' (S249A). All mutations were confirmed by sequencing. The mutant Rb (mt-Rb) cDNA was cut with BamHI, filled-in with Klenow enzyme and ligated with a ClaI linker. The ClaI fragment of mt-Rb cDNA was replaced into the Rb cDNA position of HNF1-Rb to make HNF1-mtRb. HNF1-NZ was described previously [16]. Equal amounts of HNF1-mtRb and HNF1-NZ were mixed and injected into fertilized eggs.

2.2. Western blot analysis of mt-Rb protein in HTB9 cells and liver cells

HTB9 cells were transfected with 2 μg mt-Rb expression vector. Two days after transfection, cells were collected and resuspended. Lysates were collected by centrifugation and protein concentration was determined using BCA protein assay kit (Peirce). Twenty μg of the total protein was resolved by 10% SDS–PAGE and transferred onto PVDF membranes.

Liver cells were isolated from mt-Rb transgenic and WT mice and then nuclear extracts were prepared as described previously [19]. Then lysates were recovered by centrifugation and protein concentration was determined by the same method as in culture cells. Monoclonal anti-Rb antibody (Santa Cruz, CA) was used for Western blotting analysis.

2.3. Analysis of Rb binding activity to E2F-1 by co-immunoprecipitation

HTB9 cells were co-transfected with 2 μg Rb and 4 μg E2F-1 expression vector DNAs. Two days after transfection, cells were

collected and lysed by binding buffer (10 mM Tris–HCl, pH 7.4, 150 mM NaCl, 1% Triton X-100, 1 mM EDTA, 0.3 mM PMSF, 0.5% Nonidet P-40). The lysates were collected by centrifugation and then incubated with anti-E2F-1 antibody (Santa Cruz). The immune complexes were collected on protein G Sepharose, solubilized with SDS sample buffer for immunoblotting by standard methods.

2.4. Animals, gross and histological analyses

Experimental animal protocols and animal procedures are followed with the international criteria of animal experimentation and were approved by the Hamamatsu Medical University Animal Care Center. Body weights were measured before sacrifice. Livers were obtained by autopsy, weighed and examined for the presence of tumor. For routine microscopy, Livers were fixed in 4% paraformaldehyde at 4 °C overnight for frozen section preparation and then dehydrated in 20% sucrose in PBS overnight. The specimen were frozen and sectioned at 8 μm. But for paraffin section, liver tissues were embedded in paraffin after fixation with paraformaldehyde and the sections were cut at 4 μm. Both were stained with hematoxylin and eosin according to standard methods.

2.5. Isolation of total liver mRNA and quantitative reverse transcription (qRT)-PCR assay

Total mRNA was extracted from the liver of wild type and mt-Rb transgenic mice at 11 months old using CsCl method. The quantity and quality of RNA samples were measured by absorbance at 260 and 280 nm. pRT-PCR was done as described previously [20] using the Step One Plus Real-Time PCR System (Applied Biosystems, Bedford, MA) using 24 sets of primers (Supplementary Table S1).

### 2.6. Transfection analysis of transcriptional activities of WT-Rb and mt-Rb on c-Myc promoter

PCR was performed against mouse genomic DNA with 5'-GGGATTGGTGGCTCTTGGTG-3' and 5'-CTCCCTCTGTCTCTCGCTGG as primers. The PCR product (about 2.0 kbp) was subcloned into the EcoRV site of pGL4.10 (luc2, Promega, WI) to make the c-Myc-luc2 plasmid. The fixed amount of c-Myc-luc2 plasmid and the various amounts of WT-Rb and/or mt-Rb expression vectors were cotransfected into HTB9 cells with Fugene HD (Roche). In 36 h, the cell extracts were prepared and the luciefrase activity was measured using dual luciferase system (Promega). Supplementary methods are available on line.

3. Results

3.1. Rb alanine substitution mutations and generation of mt-Rb transgenic mice

Rb contains 16 potential phosphorylation sites that are distributed among the protein [21,22] (Fig. 1A). Seven of these sites are located within C domain which is sufficient for c-Abl binding and is required for association with many non-LXCXE containing Rb-binding proteins like E2F-1 [23,24]. Two sites are located in the spacer region between A and B domains which bind the LXCXE motif and one other site is in A domain. The remaining sites are in the N-terminal region of which function is still not clear since the A, B, C and spacer domains are sufficient for activity of Rb function in most assays [25].

We mutagenized the important 12 sites out of 16 consensus sites in mt-Rb where 8 serines and 4 threonines were substituted into alanines (Fig. 1A). For in vitro analysis, the WT-Rb and mt-Rb
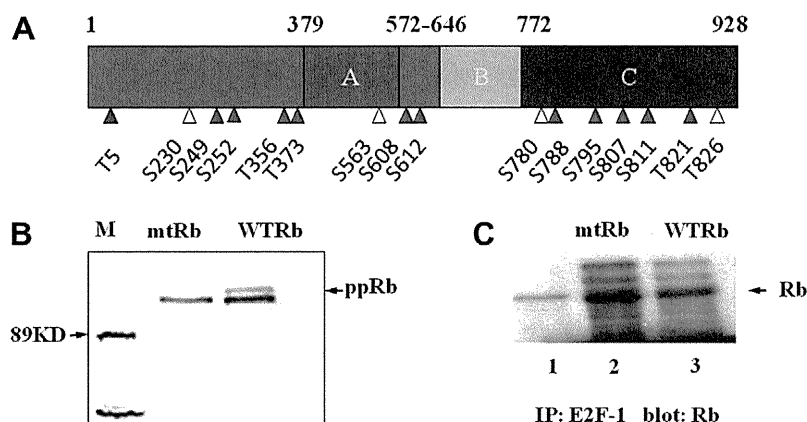
Fig. 1. Generation of phosphorylation-resistant Rb protein. (A) Schematic presentation of mutant human Rb protein. The pocket domains A, B and C were shown. Out of 16 cyclin-dependent kinase phosphorylation sites (red and white triangles), 12 sites were mutated (red triangles). (B) Phosphorylation status of WT-Rb and mt-Rb by Western blotting analysis. Phosphorylated Rb (ppRb) was detected only in cells transfected with WT-Rb expression vector (right), but not in those with mt-Rb expression vector (middle). (C) Co-immunoprecipitation of E2F1 and Rb. Cell extracts from mt-Rb expression vector-transfected cells (lane 2) and WT-Rb expression vector-transfected cells (lane 3) were incubated with anti-E2F1 antibody and the immunoprecipitates were subjected to 10% SDS–polyacrylamide gel electrophoresis. The transferred nylon membrane was incubated with anti-Rb antibody and visualized with ECL. Lane 1 shows positive control of Rb protein.

proteins were expressed in HTB9 (Rb protein-negative) cells using the cytomegalovirus enhancer/actin promoter-driven vector (CX-N2) [26]. Western blot analysis showed WT-Rb migrated as a doublet; the upper band was phosphorylated Rb protein (ppRb) and the lower band was unphosphorylated Rb protein (Fig. 1B, right lane). As compared with the wild type, the mt-Rb protein migrating in only one unphosphorylated form suggested that the mt-Rb was resistant to phosphorylation in cultured cells (Fig. 1 B, middle lane).

To confirm the E2F-1 binding activity of the mt-Rb protein, mt-Rb or WT-Rb and E2F-1 expression vectors were cotransfected into HTB9 cells. The proteins were subjected to co-immunoprecipitation and the result showed that mt-Rb bound to E2F-1 as similarly as WT-Rb did (Fig. 1C, lanes 2 and 3). This result showed that the phosphorylation site mutations did not disrupt the binding activity of mt-Rb to E2F-1.

3.2. Targeted expression of mt-Rb protein in the liver

To directly determine the effects of phosphorylation-resistant Rb on liver development and cancer progression, we generated transgenic mice in which the human mt-Rb cDNA was controlled

by the rat HNF-1 gene enhancer/promotor and obtained 2 mouse lines, TGX and TGZ. We measured the expression of Rb protein in the liver of transgenic and wild-type adult mice by Western blotting (Supplementary Fig. S1A). Large amount of mt-Rb protein was detected in the liver of TGX mice (lanes 5 and 6) and only a small amount of Rb in TGZ mice (lanes 3 and 4). In contrast, a small amount of the mouse endogenous Rb was also detected in wild-type mice (lanes 1 and 2). Next, we investigated the developmental expression pattern of β-galactosidase as an indicator of expression of mt-Rb protein by the X-gal staining. TGX embryos showed strong staining in the liver at 11.5 dpc (Supplementary Fig. S1B) while wild-type and TGZ embryos showed no staining (Supplementary Fig. S1C and data not shown). The rat endogenous HNF-1 gene is expressed in the liver, kidney, and intestine. But in our previous and current studies, 9 kbp of HNF1 promoter/enhancer directed the LacZ expression only in the liver (Fig. S1B and Ref. [16]). Furthermore, we isolated total RNA from the liver of wild-type, TGX and TGZ mice and determined whether mouse Rb (endogenous) and human Rb (exogenous) mRNAs were expressed in each liver by the RT-PCR method (Supplementary Fig. S2). The result showed that only mouse Rb mRNA was expressed in the wild-type and TGZ mice while human Rb and mouse Rb mRNAs were
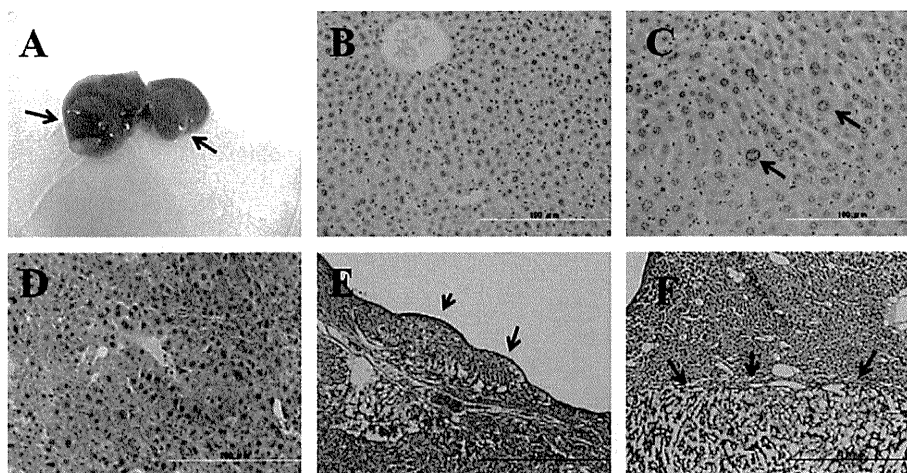
Fig. 2. Development of tumors in the liver of mt-Rb transgenic mice. (A) Macroscopic liver specimen from the mt-Rb transgenic mice at 1 year old. Tumors (adenoma) protruding from the surface of liver lobe were identified macroscopically (arrows). (B) Liver of wild-type mouse at 11 months old, 400×. (C) Liver of mt-Rb transgenic mice at 8 months. Liver cell dysplasia (large cell) was observed (arrowes), 400×. (D) Liver tumor tissue of mt-Rb transgenic mice at 11 months old. Dysplastic hepatocytes and disorganized lobular architecture were observed, 200×. (E) Multiple neoplastic nodules were observed (arrows) in the liver tumor tissue of mt-Rb mice at 11 months old, 40×. (F) A big nodule (lower part) was observed in the liver tumor tissue of mt-Rb mice at 15 months old. Arrows show a boundary between normal and tumor tissues, 40×.

expressed in TGX mice. We interpreted that the LacZ and mt-Rb genes were not expressed due to an unknown reason in the TGZ transgenic mice and investigated only the TGX transgenic mice thereafter.

3.3. Tumor development in mt-Rb transgenic mice

The liver size and architecture in the TGX transgenic mice was normal in newborns (data not shown). There were no significant differences between the mt-Rb mice and wild-type mice until 6 months old. Then the TGX mice developed hepatocyte dysplasia and foci followed by an appearance of adenomas. The incidence of

liver tumors in the TGX mice that was identified macroscopically (Fig. 2A) are summarized in Supplementary Table S2. About 50% of female and male TGX mice developed adenomas with no differences in numbers and sizes. In contrast, the age-matched B6 mice developed no adenomas.

The cell dysplasia was first noted after 8 months and the histological examination showed that some hepatocytes and nuclei were larger than normal. They had a nearly normal nuclear-cytoplasmic ratio and a pale cytoplasm (compare Fig. 2C to Fig. 2B). A prominent feature of liver tumor in the mt-Rb transgenic mice was the early development of focal lesions which was coincident with the development of the dysplastic changes. Neoplastic nodules were first
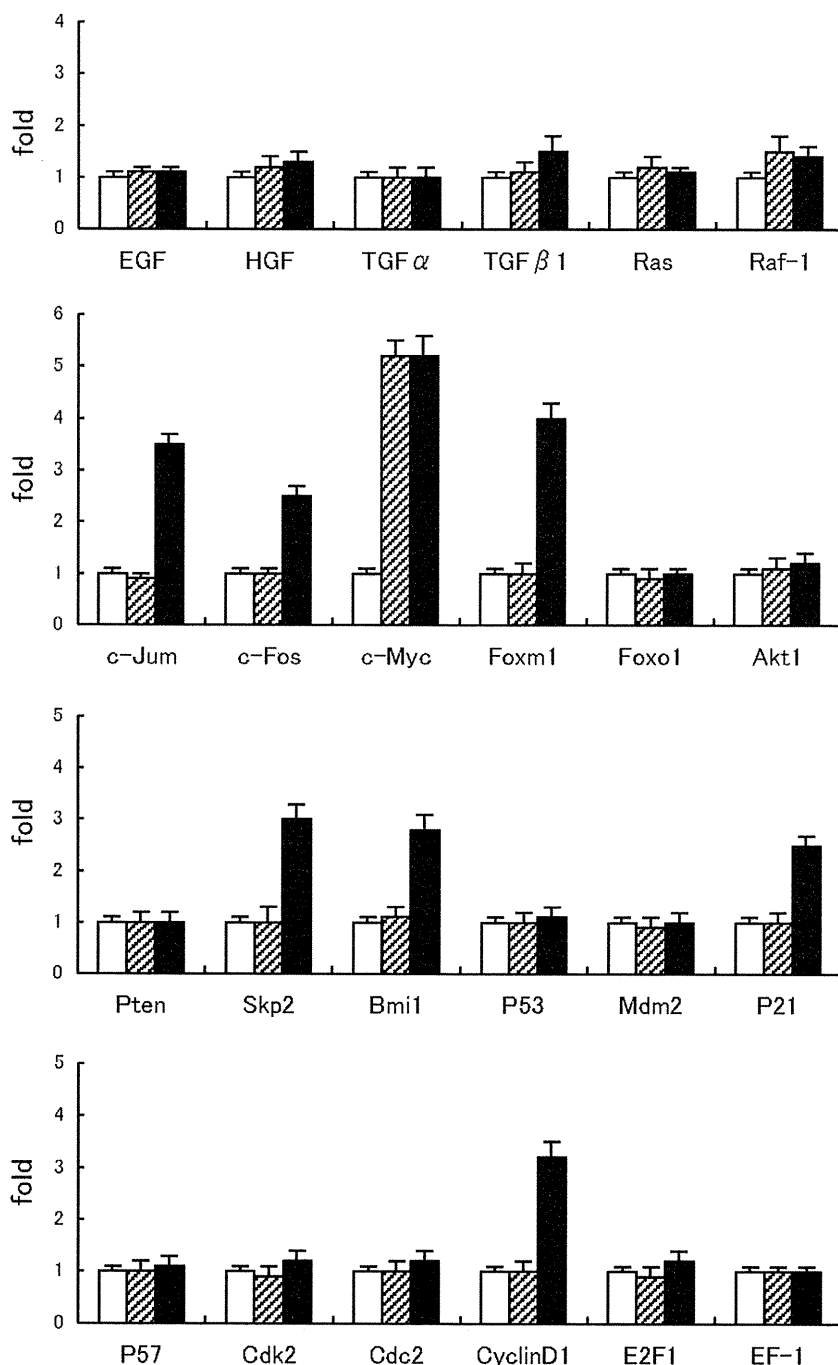
Fig. 3. qRT-PCR analysis of gene expression in the liver of transgenic mice. Total RNA was isolated from the liver of wild-type (open bars) and the mt-Rb transgenic mice without macroscopic tumors (shadowed bars) and those with macroscopic tumors (filled bars) at the age of 11 months and amplified quantitatively with a set of primers for each mRNA (n = 5).

noted in the liver of mt-Rb transgenic mice after 11 months. Microscopic examination showed the neoplastic nodules were composed of trabecular hepatocytes, arranged in sheets and cords which resemble normal hepatocytes but have some deviations in cell and nuclear size (larger cell), and were lacking of lobular architectures (Fig. 2D). Lower magnification view of the liver tissue from 11 months old (Fig. 2E) and 15 months old (Fig. 2F) transgenic mice showed the interface between the tumor which contained multiple nodules and septa, and the hepatic parenchyma which has no fibrosis and cirrhosis. Macroscopically, the livers contained solitary nodules of relatively small size bulging from the surface of the liver (Fig. 2A). Over all, both these foci and visible neoplasms had the characteristics of hepatocellular adenoma.

3.4. Gene expression in the transgenic mouse liver

To know the molecular mechanism of the tumor formation in mt-Rb transgenic mice, we determined whether the gene expression pattern was altered or not. qRT-PCR analyses of whole liver revealed that c-Myc mRNA was dramatically up-regulated in both non-tumorous and tumorous livers of mt-Rb transgenic mice compared with WT mice (Fig. 3). Only in tumorous liver, Foxm1, Bmi1, c-Jun, c-Fos, and Skp2 were also up-regulated. These results suggested that the constituted expression of mt-Rb can up-regulate the expression of c-Myc. Therefore, the tumorigenesis was significantly induced when the other genes mentioned above were up-regulated.

In the tumorous liver of mt-Rb transgenic mice, P21 mRNA was up-regulated. This result suggested that apoptosis might be enhanced due to an increase of P21 during liver tumorigenesis in the transgenic mice. Furthermore, several cell cycle-related genes, such as CyclinD1, was up-regulated in the tumors. In contrast, EGF, HGF, TGFα, TGFβ, Ras, Raf-1, Foxo1, Akt1, Pten, p53, Mdm2, p57, Cdk2, and E2F-1 mRNAs had no significant changes (Fig. 3).

3.5. Mutant Rb protein reversed the repression of the wild-type Rb protein onto Myc gene

All mt-Rb transgenic mice showed up-regulation of c-Myc mRNA in the liver. So we investigated whether the mt-Rb protein activated the c-Myc gene. We connected the promoter region of c-Myc gene to the luciferase gene to make the c-Myc-luc2 construct.

Various amounts of WT-Rb and mt-Rb expression vectors were cotransfected into HTB9 cells and the luciferase activities were measured. The WT-Rb proteins repressed the c-Myc promoter

dramatically while the mt-Rb protein repressed very weakly (Fig. 4A). Next, we transfected various amounts of mt-Rb expression vector with a fixed amount of WT-Rb expression vector into HTB9 cells. Interestingly, the mt-Rb protein inhibited the repression of WT-Rb protein (Fig. 4B). This result indicates that mt-Rb acts as an inhibitor to WT-Rb.

4. Discussion

Here we report that targeted expression of mt-Rb in the mouse liver exhibited macroscopic neoplastic nodules with about 50% incidence within 15 months old. These tumorous tissues had the characteristics of hepatocellular adenoma. Rb is the first-identified human tumor suppressor gene, and many lines of evidence have shown that loss or inactivation of Rb is an obligatory step in tumor formation. Paradoxically, Rb also has an apoptosis inhibition function. Since a defect in apoptosis is one of well-known oncogenic mechanisms, this functional property predicts that deregulated Rb expression may be oncogenic [27]. This concept is supported by the observations made in mice that express phosphorylation-resistant Rb in the mammary gland [28], and that express caspase-resistant Rb in p53-null knockout mice [29]. In addition to the inhibition of apoptosis, it is conceivable that constitutively active Rb may result in the accumulation of damaged DNA and the acquisition of transforming mutations [28]. These and our results suggest that the constitutively active Rb protein might have an oncogenic character.

Intriguingly, we found that the level of c-Myc mRNA was dramatically increased in both tumorous and non-tumorous livers of 11 months old transgenic mice compared with WT mice. Recently, it has been shown that a complex cross-regulation between Myc and Rb is mediated through the control of E2F in MYC-induced T cell lymphomagenesis [30]. Another study showed that down-regulation of MYC can activate Rb pathway through CDK4 and p15^{INK4b} in STAT5A-induced senescence [31]. Consistent with these reports, our results may raise the possibility of derepressive activity of mt-Rb on WT-Rb on the Myc promoter (Fig. 4B). Up-regulation of c-Myc mRNA in non-tumorous liver suggests that the c-Myc up-regulation by itself does not cause a tumor formation.

It has been reported that c-Myc binds to an E-box of Foxm1 promoter and up-regulates the expression of Foxm1 in the liver [32,33]. Furthermore, c-Myc regulates multiple target genes including c-Jun, Bmi1, CyclinD1 and TGFβ1 [32]. Another important finding of our study is the dramatic up-regulation of Foxm1 mRNA in the tumor in the mt-Rb transgenic liver. Foxm1 works as a cell cycle regulator, especially at S and G2/M phases [34]. Foxm1
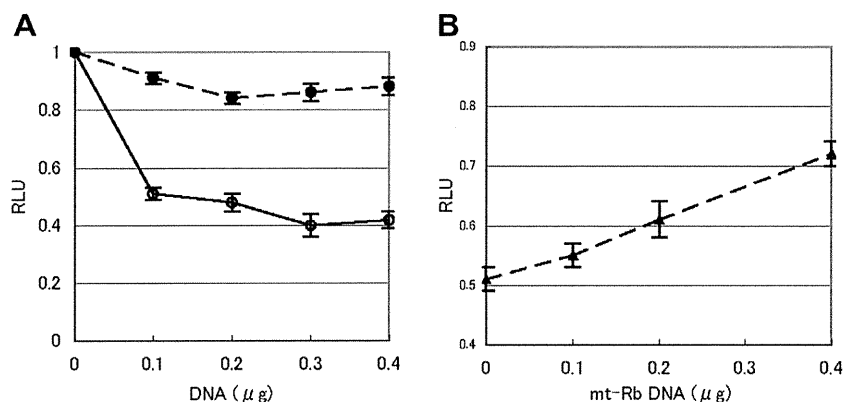
Fig. 4. mt-Rb reversed the repression to c-Myc promoter by WT-Rb. (A) The fixed amount (0.2 μg) of Myc-luc2 plasmid and various amounts of WT-Rb (solid line) or mt-Rb (broken line) expression vector were cotransfected into HTB9 cells. In 36 h, the cell extracts were prepared and the luciferase activities were measured and expressed as Mean ± SD (n = 3). (B) The Myc-luc2 plasmid (0.2 μg), WT-Rb expression vector (0.2 μg) and various amounts of mt-Rb expression vectors were cotransfected into HTB9 cells. The luciferase activity of cell extracts was measured and expressed as Mean ± SD (n = 3).

increases expression of numerous mitotic genes, such as *Cyclin A2, Cdc 25B phosphatase, CyclinB1* and *Skp2*, and down-regulates *P21* and *P27* [34]. However, *Foxm1* is not the only c-Myc target gene, and many of the cell cycle genes downstream of *Foxm1* have also been shown to be direct targets of c-Myc [33,35,36]. Our result showed that up-regulation of *c-Myc* target genes, *Foxm1, Bmi1, Skp2, AP-1(c-Jun/c-Fos)* and *CyclinD1*, was observed only in the tumors of mt-Rb liver. Bmi1, Skp2, AP-1 and CyclinD1 are known to be involved in oncogenesis [37–40]. In summary, the over-expression of phosphorylation-resistant Rb resulted in liver tumor formation. Our results suggest that the continued high expression of several c-Myc target genes promotes the liver tumor formation.

5. Conflict of interest statement

None.

Acknowledgment

Appendix A. Supplementary data

Supplementary data associated with this article can be found, in the online version, at doi:10.1016/j.bbrc.2011.12.014.

References

[1] D. Motola-Kuba, D. Zamora-Valdes, M. Uribe, N. Mendez-Sanchez, Hepatocellular carcinoma. An overview, An. Hepatol. 5 (2006) 16–24.
[2] H. Blum, Hepatocellular carcinoma: therapy and prevention, World J. Gastroenterol. 11 (2005) 7391–7400.
[3] E.K. Teo, K.M. Fock, Hepatocellular carcinoma: an Asian perspective, Dig. Dis. 19 (2001) 263–268.
[4] R.N. Aravalli, C.J. Steer, E.N. Cressman, Molecular mechanisms of hepatocellular carcinoma, Hepatology 48 (2008) 2047–2063.
[5] P.E. Zondervan, J. Wink, J.C. Alers, et al., Molecular cytogenetic evaluation of virus-associated and non-viral hepatocellular carcinoma: analysis of 26 carcinomas and 12 concurrent dysplasias, J. Pathol. 192 (2000) 207–215.
[6] W. Du, J. Pogoriler, Retinoblastoma family genes, Oncogene 25 (2006) 5190–5200.
[7] G. Scambia, S. Lovergine, V. Masciullo, RB family members as predictive and prognostic factors in human cancer, Oncogene 25 (2006) 5302–5308.
[8] D.H. Abramson, R.M. Ellsworth, F.D. Kitchin, G. Tung, Second nonocular tumors in retinoblastoma survivors. Are they radiation-induced?, Ophthalmology 91 (1984) 1351–1355.
[9] M.F. Hansen, A. Koufos, B.L. Gallie, et al., Osteosarcoma and retinoblastoma: a shared chromosomal mechanism revealing recessive predisposition, Proc. Natl. Acad.Sci. USA 82 (1985) 6216–6220.
[10] J.W. Harbour, S.L. Lai, J. Whang-Peng, A.F. Gazdar, J.D. Minna, F.J. Kaye, Abnormalities in structure and expression of the human retinoblastoma gene in SCLC, Science 241 (1988) 353–357.
[11] Y. Kubota, K. Fujinami, H. Uemura, et al., Retinoblastoma gene mutations in primary human prostate cancer, Prostate 27 (1995) 314–320.
[12] E.Y. Lee, H. To, J.Y. Shew, R. Bookstein, P. Scully, W.H. Lee, Inactivation of the retinoblastoma susceptibility gene in human breast cancers, Science 241 (1988) 218–221.
[13] H. Miyamoto, T. Shuin, S. Torigoe, Y. Iwasaki, Y. Kubota, Retinoblastoma gene mutations in primary human bladder cancer, Br. J. Cancer 71 (1995) 831–835.
[14] A. Teufel, F. Staib, S. Kanzler, A. Weinmann, H. Schulze-Bergkamen, P.R. Galle, Genetics of hepatocellular carcinoma, World J. Gastroenterol. 13 (2007) 2271–2282.
[15] A.M. Hui, X. Li, M. Makuuchi, T. Takayama, K. Kubota, Over-expression and lack of retinoblastoma protein are associated with tumor progression and metastasis in hepatocellular carcinoma, Int. J. Cancer 84 (1999) 604–608.
[16] T. Ichihara, Y. Komagata, X.L. Yang, et al., Resistance to fulminant hepatitis and carcinogenesis conferred by overexpression of retinoblastoma protein in mouse liver, Hepatology 33 (2001) 948–955.
[17] C.N. Mayhew, E.E. Bosco, S.R. Fox, et al., Liver-specific pRB loss results in ectopic cell cycle entry and aberrant ploidy, Cancer Res. 65 (2005) 4568–4577.
[18] S. Barrientes, C. Cooke, D.W. Goodrich, Glutamic acid mutagenesis of retinoblastoma protein phosphorylation sites has diverse effects on function, Oncogene 19 (2000) 562–570.
[19] H. Yamada, S. Hirai, S. Ikegami, Y. Kawarada, E. Okuhara, H. Nagano, The fate of DNA originally existing in the zygote nucleus during achromosomal cleavage of fertilized echinoderm eggs in the presence of aphidicolin: microscopic studies with anti-DNA antibody, J. Cell Physiol. 124 (1985) 9–12.
[20] R. Pascale, M.M. Simile, D.F. Calvisi, et al., Role of HSP90, CDC37, and CRM1 as modulators of p16^{INK4A} activity in rat liver carcinogenesis and human liver cancer, Hepatology 42 (2005) 1310–1319.
[21] A.S. Lundberg, R.A. Weinberg, Functional inactivation of the retinoblastoma protein requires sequential modification by at least two distinct cyclin-cdk complexes, Mol. Cell Biol. 18 (1998) 753–761.
[22] S. Mittnacht, Control of pRB phosphorylation, Curr. Opin. Genet. Dev. 8 (1998) 21–27.
[23] X.Q. Qin, T. Chittenden, D.M. Livingston, W.G. Kaelin Jr., Identification of a growth suppression domain within the retinoblastoma gene product, Genes. Dev. 6 (1992) 953–964.
[24] S. Huang, E. Shin, K.A. Sheppard, et al., The retinoblastoma protein region required for interaction with the E2F transcription factor includes the T/E1A binding and carboxy-terminal sequences, DNA Cell Biol. 11 (1992) 539–548.
[25] S. Huang, N.P. Wang, B.Y. Tseng, W.H. Lee, E.H. Lee, Two distinct and frequently mutated regions of retinoblastoma protein are required for binding to SV40 T antigen, EMBO J. 9 (1990) 1815–1822.
[26] H. Niwa, K. Yamamura, J. Miyazaki, Efficient selection for high-expression transfectants with a novel eukaryotic vector, Gene 108 (1991) 193–199.
[27] D.W. Goodrich, The retinoblastoma tumor-suppressor gene, the exception that proves the rule, Oncogene 25 (2006) 5233–5243.
[28] Z. Jiang, E. Zacksenhaus, Activation of retinoblastoma protein in mammary gland leads to ductal growth suppression, precocious differentiation, and adenocarcinoma, J. Cell Biol. 156 (2002) 185–198.
[29] H.L. Borges, J. Bird, K. Wasson, et al., Tumor promotion by caspase-resistant retinoblastoma protein, Proc. Natl. Acad. Sci. USA 102 (2005) 15587–15592.
[30] R. Opavsky, S.Y. Tsai, M. Guimond, et al., Specific tumor suppressor function for E2F2 in Myc-induced T cell lymphomagenesis, Proc. Natl. Acad. Sci. USA 104 (2007) 15400–15405.
[31] F.A. Mallette, M.F. Gaumont-Leclerc, G. Huot, G. Ferbeyre, Myc down-regulation as a mechanism to activate the Rb pathway in STAT5A-induced senescence, J. Biol. Chem. 282 (2007) 34938–34944.
[32] P.C. Fernandez, S.R. Frank, L. Wang, et al., Genomic targets of the human c-Myc protein, Genes Dev. 17 (2003) 1115–1129.
[33] W.E. Blanco-Bose, M.J. Murphy, A. Ehninger, et al., C-Myc and its target FoxM1 are critical downstream effectors of constitutive androstane receptor (CAR) mediated direct liver hyperplasia, Hepatology 48 (2008) 1302–1311.
[34] J. Laoukili, M. Stahl, R.H. Medema, FoxM1: at the crossroads of aging and cancer, Biochim. Biophys. Acta 1775 (2007) 92–102.
[35] Q.M. Guo, R.L. Malek, S. Kim, et al., Identification of c-Myc responsive genes using rat cDNA microarray, Cancer Res. 60 (2000) 5922–5928.
[36] Z. Li, S. VanCalcar, C. Qu, W.K. Cavenee, M.Q. Zhang, B. Ren, A global transcriptional regulatory role for c-Myc in Burkitt's lymphoma cells, Proc. Natl. Acad. Sci. USA 100 (2003) 8164–8169.
[37] J.S. Dovey, S.J. Zacharek, C.F. Kim, J.A. Lees, Bmi1 is critical for lung tumorigenesis and bronchioalveolar stem cell expansion, Proc. Natl. Acad. Sci. USA 105 (2008) 11857–11862.
[38] M. Gstaiger, R. Jordan, M. Lim, C. Catzavelos, J. Mestan, J. Slingerland, Skp2 is oncogenic and overexpressed in human cancers, Proc. Natl. Acad. Sci. USA 98 (2001) 5043–5048.
[39] R. Eferl, E.F. Wagner, AP-1: a double-edged sword in tumorigenesis, Nat. Rev. Cancer 3 (2003) 859–868.
[40] H. Yamamoto, T. Ochiya, F. Takeshita, et al., Enhanced skin carcinogenesis in cyclin D1-conditional transgenic mice: cyclin D1 alters keratinocyte response to calcium-induced terminal differentiation, Cancer Res. 62 (2002) 1641–1647.

VEGFR-3 controls tip to stalk conversion at vessel fusion sites by reinforcing Notch signalling

Tuomas Tammela[1,9], Georgia Zarkada[1,9], Harri Nurmi[1], Lars Jakobsson[2,10], Krista Heinolainen[1], Denis Tvorogov[1], Wei Zheng[1], Claudio A. Franco[2], Aino Murtomäki[1], Evelyn Aranda[3], Naoyuki Miura[4], Seppo Ylä-Herttuala[5], Marcus Fruttiger[6], Taija Mäkinen[1,10], Anne Eichmann[7], Jeffrey W. Pollard[3], Holger Gerhardt[2,8], and Kari Alitalo[1,11]

[1]Molecular/Cancer Biology Laboratory, Institute for Molecular Medicine Finland, Research Programs Unit and Department of Pathology, Haartman Institute, Biomedicum Helsinki, PO Box 63 (Haartmaninkatu 8), 00014 University of Helsinki, Finland [2]Vascular Biology Laboratory, London Research Institute—Cancer Research UK, 44 Lincoln's Inn Fields, London WC2A 3PX, UK [3]Department of Developmental and Molecular Biology, Albert Einstein College of Medicine, New York, New York 10461, USA [4]Department of Biochemistry, Hamamatsu University School of Medicine, 431-3192 Hamamatsu, Japan [5]A. I. Virtanen Institute and Department of Medicine, University of Kuopio, PO Box 1627, 70211 Kuopio, Finland [6]Institute of Ophthalmology, University College London, London EC1V 9EL, UK [7]Institut National de la Santé et de la Recherche Médicale U833, Collège de France, 11 Place Marcelin Berthelot, 75005 Paris, France [8]Vascular Patterning Laboratory, Vesalius Research Center, VIB, Campus Gasthuisberg, B-3000 Leuven, Belgium

Abstract

Angiogenesis, the growth of new blood vessels, involves specification of endothelial cells to tip cells and stalk cells, which is controlled by Notch signalling, whereas vascular endothelial growth factor receptor (VEGFR)-2 and VEGFR-3 have been implicated in angiogenic sprouting. Surprisingly, we found that endothelial deletion of *Vegfr3*, but not VEGFR-3-blocking antibodies, postnatally led to excessive angiogenic sprouting and branching, and decreased the level of Notch signalling, indicating that VEGFR-3 possesses passive and active signalling modalities.

Furthermore, macrophages expressing the VEGFR-3 and VEGFR-2 ligand VEGF-C localized to vessel branch points, and *Vegfc* heterozygous mice exhibited inefficient angiogenesis characterized by decreased vascular branching. FoxC2 is a known regulator of Notch ligand and target gene expression, and *Foxc2*^{+/−}; *Vegfr3*^{+/−} compound heterozygosity recapitulated homozygous loss of *Vegfr3*. These results indicate that macrophage-derived VEGF-C activates VEGFR-3 in tip cells to reinforce Notch signalling, which contributes to the phenotypic conversion of endothelial cells at fusion points of vessel sprouts.

During late embryogenesis and in the adult, blood vessels form primarily by angiogenesis, that is by sprouting from pre-existing vessels. Vascular endothelial growth factor (VEGF) potently promotes angiogenesis, and is indispensable for vascular development[1,2], and VEGFR-2 tyrosine kinase is the primary receptor transmitting VEGF signals in endothelial cells[3,4]. VEGFR-3 is activated by the VEGF homologues VEGF-C and VEGF-D, which, when fully proteolytically processed, also stimulate VEGFR-2 (ref. 5) and induce the formation and activation of VEGFR-2–VEGFR-3 heterodimers[6,7]. Inactivation of the *Vegfr3* gene (also known as *Flt4*) leads to marked defects in arterial–venous remodelling of the primary vascular plexus, resulting in lethality by embryonic day (E) 10.5 (ref. 8) or to defective segmental artery morphogenesis[9] in mice or zebrafish, respectively.

As the lymphatic vessels begin to develop at around E10.5, the level of *Vegfr3* expression gradually decreases in the blood vessels, and from E16.5 onwards it is found nearly exclusively in the lymphatic vascular endothelium[10,11]. However, VEGFR-3 is induced in angiogenic endothelial cells for example in tumours, wounds and in maturing ovarian follicles[12–14]. Homozygous gene-targeting of *Vegfc* leads to embryonic lethality at E16.5 due to a complete failure in lymphatic vessel formation, whereas *Vegfc* heterozygous mice survive with lymphatic vessel hypoplasia and lymphedema, but do not exhibit blood vascular defects as adults[15]. Conversely, *Vegfd* gene-targeted mice are viable and normal[16]. Interestingly, compound deletion of both *Vegfc* and *Vegfd* phenocopies the homozygous loss of *Vegfc*, but these mice survive past the time point of critical requirement for *Vegfr3* (ref. [17]), implicating other as yet unknown ligands or ligand-independent signalling for VEGFR-3.

Angiogenic sprouting involves specification of subpopulations of endothelial cells into tip cells that respond to VEGF guidance cues, and stalk cells that follow the tip cells and proliferate to form the vascular network[18]. Recent evidence indicates that VEGF induces the membrane-bound Notch ligand delta-like 4 (Dll4) in the tip cells, which leads to the induction of the stalk-cell phenotype in adjacent endothelial cells through activation of Notch-1 (refs 10,19–21). The angiogenic sprouts fuse at intervals[18], followed by the formation of a vessel lumen to form a functional microcirculatory loop[22,23]. The fusion of migrating tip cells is chaperoned by Tie2- and neuropilin-1-positive macrophages[24], which express a variety of growth factors and proteolytic enzymes[24–26]. However, the molecular players regulating sprout fusion and vessel anastomosis have remained unknown.

We recently demonstrated that VEGFR-3 is expressed at a high level in endothelial tip cells, and that blocking VEGFR-3 with antibodies results in decreased angiogenesis during postnatal development and in tumours[14]. Stimulation of VEGFR-3 augments VEGF-induced angiogenesis and sustains blood vessel growth even in the presence of VEGFR-2 inhibitors, whereas antibodies against VEGFR-3 and VEGFR-2 in combination produce additive inhibition of angiogenesis and tumour growth[14]. Consistent with the concept of high levels of VEGFR-3 activity in the tip cells, genetic or pharmacological disruption of the Notch signalling pathway *in vivo* leads to widespread endothelial *Vegfr3* expression and excessive sprouting[14,27,28].

Here, we show that genetic inactivation of *Vegfr3* in endothelial cells surprisingly resulted in increased numbers of tip cells and vessel hyperplasia, which closely resembled loss of Notch signalling, whereas haploinsufficiency of *Vegfc* led to disruption of tip cell fusion points and inefficient angiogenesis. Our results implicate a bimodal role for VEGFR-3 in regulating angiogenesis, and indicate that the VEGF-C–VEGFR-3 signalling pathway controls the branching morphogenesis of blood vessels.

RESULTS

Endothelial deletion of *Vegfr3* results in excessive angiogenesis

To study the consequences of homozygous endothelial-specific loss of *Vegfr3* during angiogenesis, we mated *Vegfr3$^{flox/flox}$* mice with *PdgfbiCreER^{T2}* mice that express tamoxifen-activated Cre recombinase in endothelial cells[29]. Complete deletion of *Vegfr3* in the retinal endothelium was achieved by 24 h following administration of 4-hydroxytamoxifen (4-OHT; Supplementary Fig. S1a–d). Some residual *Vegfr3* expression was detected by quantitative real-time (qRT) PCR (Supplementary Fig. S1e), presumably originating from retinal oligodendrocytes[30] or from monocytic cells[31].

Surprisingly, when Cre was induced in *PdgfbiCreER^{T2}*; *Vegfr3$^{flox/flox}$* (*Vegfr3^{iΔEC}*) mice for 48 h from postnatal day (P) 3 to P5, marked excessive branching, filopodia projection and hyperplasia of the nascent vascular plexus were observed (Fig. 1a–e). There was a significant increase in the proliferation of retinal endothelial cells (Fig. 1f and Supplementary Fig. S2). Increased branching and vascular hyperplasia were also observed in hindbrains of *Vegfr3^{iΔEC}* embryos at E11.5 (Fig. 1g–k and Supplementary Fig. S3).

We sought to validate these findings in other models outside the developing central nervous system. Excessive angiogenesis and sprouting were also detected in syngeneic subcutaneously implanted Lewis lung carcinomas (LLC) and B16-F10 melanomas in the *Vegfr3^{iΔEC}* mice (Fig. 1l,m and data not shown). Furthermore, when ears of adult *Vegfr3^{iΔEC}* mice were transduced with AdVEGF, we observed a more robust angiogenic response, characterized by increased vascular tortuosity, enlargement and surface area (Fig. 1n and Supplementary Fig. S4).

VEGFR-3 tyrosine kinase activity is crucial for lymphatic vessel growth[32], but its role in angiogenesis is not known. To determine whether VEGFR-3 is tyrosine phosphorylated in blood vascular endothelial cells *in vivo*, we injected recombinant VEGF, VEGF-C or BSA control protein into the outflow tract of wild-type embryos at E10.5, a stage when lymphatic vessels have not yet developed (Fig. 2a–c). VEGF did not promote tyrosine phosphorylation of VEGFR-3, unlike VEGF-C, but a faint phosphorylation signal was detected in both VEGF- and BSA-stimulated embryos, indicating a baseline level of VEGFR-3 phosphorylation (Fig. 2b). As expected, VEGF and VEGF-C both stimulated VEGFR-2 phosphorylation (Fig. 2c).

We have previously shown that VEGFR-3-blocking antibodies suppress angiogenesis[14], whereas our results surprisingly showed that genetic targeting of *Vegfr3* produced excessive angiogenic sprouting, indicating the possibility of ligand-independent sprouting. We found that VEGFR-3 was phosphorylated in the absence of its ligands by stimulation with collagen I in cultured human dermal blood vascular endothelial cells (hBECs) even in the presence of blocking monoclonal antibodies or a VEGFR tyrosine kinase inhibitor, whereas the Src inhibitor PP2 blocked collagen-I-induced phosphorylation of VEGFR-3 (Fig. 2d), indicating that VEGFR-3 can be phosphorylated independently of its ligands[33].

We addressed the role of VEGFR-3 kinase activity in angiogenesis *in vivo* by studying the retinas of *Chy* mice, which harbour a heterozygous kinase-inactivating point mutation in the tyrosine kinase domain (*Vegfr3$^{KD/+}$*), leading to a decreased level of VEGFR-3 signalling and severe lymphatic vessel hypoplasia[32]. The retinas of mice harbouring one kinase-dead (KD) and one deleted *Vegfr3* allele (*Vegfr3$^{i\Delta EC/KD}$*) showed an increase in the vascular area, branching and filopodia projection that was comparable to homozygous loss of *Vegfr3* (*Vegfr3$^{i\Delta EC/i\Delta EC}$*; Fig. 2e–i), indicating that VEGFR-3 hypophosphorylation can trigger the phenotype. In contrast, *Vegfr3$^{KD/+}$* and *Vegfr3$^{i\Delta EC/+}$* single heterozygotes were indistinguishable from wild-type retinas (Fig. 2e–i).

The administration of VEGFR-3-blocking antibodies to *Vegfr3$^{i\Delta EC}$* mice did not affect the hypervascular phenotype (Fig. 3a,b). In contrast, VEGFR-2-blocking antibodies rescued the increase in vascular area in the *Vegfr3$^{i\Delta EC}$* mice (Fig. 3a,b). However, the nascent vessels appeared abnormally thick in the *Vegfr3$^{i\Delta EC}$* retinas following administration of VEGFR-2-blocking antibodies (arrowheads in Fig. 3a), indicating that the phenotypic rescue was not complete. Furthermore, the expression level of VEGFR-1, a negative regulator of VEGF, was decreased in the *Vegfr3$^{i\Delta EC}$* retinas (Fig. 3c), indicating an increased level of VEGF–VEGFR-2 signalling. Consistently, we detected a minor increase in the level of VEGFR-2 phosphorylation following stimulation of cultured human umbilical vein endothelial cells (HUVECs) with VEGF when VEGFR-3 expression was silenced using siRNA oligonucleotides (Fig. 3d). Antibodies blocking human VEGFR-3 had no effect on VEGFR-2 phosphorylation in response to VEGF in HUVECs (Supplementary Fig. S5a).

Loss of *Vegfr3* in endothelial cells leads to a decreased level of Notch target gene expression

The phenotype resulting from endothelial *Vegfr3* deletion closely resembled the hyperplastic vascular pattern resulting from inhibition of Dll4/Notch signalling between tip and stalk cells. Indeed, we detected a marked decrease in the level of Notch target gene transcripts and the Notch ligand *Dll4* in the *Vegfr3$^{i\Delta EC}$* retinas (Fig. 4a), indicating a decreased level of Notch signalling in the endothelium, resulting in tip cell dominance over stalk cells. In contrast, no changes in Notch targets could be observed in pups treated with VEGFR-3-blocking antibodies (Supplementary Fig. S5b), indicating that the perturbations to VEGFR-3 by blocking antibodies and genetic targeting are qualitatively different.

To investigate the responsiveness of the *Vegfr3*-deficient endothelium to exogenous Notch activation, we administered Jagged1, a small peptide Notch agonist, to *Vegfr3$^{i\Delta EC}$* pups, and observed a rescue of the hypervascular phenotype (Fig. 4b,c). Notably, the vasculature was normalized also in terms of morphology, unlike after anti-VEGFR-2 antibody administration (Fig. 4c), indicating that decreased Notch signalling underlies the phenotype in *Vegfr3$^{i\Delta EC}$* retinas.

According to our results, VEGFR-3 contributes to the activation of Notch that is known to promote a phenotypic switch from a tip cell to a stalk cell. We chose to test this hypothesis in mosaic embryoid bodies consisting of both *Vegfr3$^{+/LacZ}$* heterozygous and wild-type embryonic stem cells[34]. *Vegfr3$^{+/LacZ}$* endothelial cells preferentially localized to the tips of VEGF-induced vascular sprouts (Fig. 4d,g), whereas inhibiting Notch cleavage with the γ-secretase inhibitor DAPT abrogated the competitive advantage of the *Vegfr3$^{+/LacZ}$* endothelial cells (Fig. 4h). *Vegfr3$^{+/LacZ}$* endothelial cells preferentially localized to the tips of vascular sprouts also in mosaic retinas at P5 (Fig. 4i), indicating increased tip cell competence for the *Vegfr3* haploinsufficient cells, which further implicates a decreased level of Notch signalling in endothelial cells with targeted *Vegfr3* loss-of-function.

VEGF-C–VEGFR-3 signalling controls fusion of vascular sprouts

We next sought to determine which of the two VEGFR-3 ligands, VEGF-C or VEGF-D, is responsible for activating VEGFR-3 in the angiogenic endothelium *in vivo*. Strikingly, *Vegfc* heterozygous mice demonstrated retardation of retinal vascularization and decreased vessel branching density (Fig. 5a–d). In contrast, the *Vegfc* heterozygotes exhibited increased vessel sprouting and filopodia projection (Fig. 5e,f), and a decrease in the level of Notch target gene expression (Fig. 5g). These results implied a failure in stabilization of sprout fusion sites, and indicated that the excess sprouts represent failed tip cell fusions. Indeed, tracking endothelial cell migration paths by collagen IV immunostaining showed that endothelial cells in *Vegfc*-haploinsufficient mice had frequently retracted from putative sprout fusion sites (Fig. 5h,i). Importantly, *Vegf* (also known as *Vegfa*) levels in the *Vegfc* heterozygous retinas were normal, whereas *Vegfc* transcript levels were decreased by more than 50% (Supplementary Fig. S5c). No changes in angiogenesis were observed in homozygous or heterozygous *Vegfd* gene-targeted retinas (Supplementary Fig. S6), indicating that VEGF-C is the key ligand responsible for VEGFR-3 activation during retinal angiogenesis.

Macrophages expressing Tie2 have been implicated as critical cellular chaperones for the formation of vascular anastomoses[24,25], and our results indicated a role for VEGF-C in this process. We detected VEGF-C expression in 50.9% (3.1% ± s.e.m.) of F4/80-positive macrophages in wild-type retinas. High-resolution imaging showed that all F4/80- and Tie2-positive cells were also VEGF-C positive (Fig. 5j). Curiously, the VEGF-C-positive macrophages were positioned at the vascular front and primarily resided at vascular branching points immediately behind the tip cell front, whereas macrophages at sites of tip cell engagement expressed lower levels of VEGF-C (Fig. 5j and Supplementary Fig. S7).

Interestingly, complete loss of macrophages in *op/op* mice[35] largely phenocopied heterozygous loss of *Vegfc*, as evidenced by decreased radial migration, area and branching of the vascular plexus, as well as by increased sprouting of the vessels (Fig. 5k–o). Furthermore, the Notch target genes *Hey1* and *Hey2* were significantly downregulated in the *op/op* retinas (Fig. 5p).

VEGF-C–VEGFR-3 signals induce Notch target genes through PI(3)K and FOXC2

To understand the mechanisms whereby VEGF-C–VEGFR-3 signalling contributes to Notch signalling, we stimulated cultured hBECs with VEGF-C and observed induction of Notch target genes over a 1–2 h stimulation period (Fig. 6a and data not shown). We found that VEGF-C induced *DLL4* in the hBECs (Supplementary Fig. S8), but similar induction of the Notch targets was observed also in the presence of a soluble Notch inhibitor, Dll4-Fc (Fig. 6a), implicating ligand-independent induction of Notch targets. Silencing VEGFR-3 expression with siRNA suppressed the induction of Notch targets and *DLL4* in response to VEGF-C (Fig. 6b). Interestingly, VEGF-C potentiated Notch target gene expression induced by transduction of hBECs with a retrovirus encoding membrane-bound Dll4 (Fig. 6c). The endothelial Notch receptors (*NOTCH1* and *NOTCH4*) were not induced by VEGF-C stimulation (Supplementary Fig. S8). Taken together, these data indicate that VEGF-C–VEGFR-3 signalling can induce Notch target genes through a mechanism that is independent of canonical Notch signalling.

Phosphatidylinositol 3-kinase (PI(3)K) is a downstream effector of receptor tyrosine kinases, and it has been implicated as a positive regulator of Notch signalling[36–38]. PI(3)K is activated by VEGFR-3 signals, indicating a mechanism for activation of Notch downstream of VEGFR-3. Indeed, pharmacological inhibition of PI(3)K, but not the MAP-kinase MEK, suppressed Notch activation by VEGF-C (Fig. 6d and data not shown). Interestingly, siRNA

silencing of VEGFR-3 expression returned ligand-induced activation of PI(3)K to baseline levels (Fig. 6e), indicating that PI(3)K activity is at least partially regulated by VEGFR-3 in angiogenic endothelial cells.

PI(3)K/Akt signalling is known to regulate FOX family transcription factors[39], and VEGFR-3 has been reported to genetically interact with FoxC2 in lymphatic endothelial cells[40]. FOXC2 has also been shown to directly regulate *HEY2* and *DLL4* expression[38,41], indicating a possible link between the VEGFR-3 and Notch signalling pathways. We found *FOXC2* messenger RNA induction in hBECs by VEGF-C stimulation, but not in response to Notch activation by membrane-bound Dll4 (Fig. 7a and data not shown). Loss of *Vegfr3 in vivo* led to a marked decrease in the level of FoxC2 expression in the endothelial cells at the angiogenic front (Fig. 7b–d). Downregulation of *Foxc2* was also evident in *Vegfc* heterozygous retinas (Fig. 7e). To investigate whether VEGFR-3 and FoxC2 function in the same pathway, we generated *Vegfr3*$^{+/-}$;*Foxc2*$^{+/-}$ compound heterozygous mice, which exhibited similar excessive endothelial growth, branching and filopodia projection as observed in the *Vegfr3*$^{i\Delta EC}$ homozygous retinas (Figs 7f–i, 1). The vasculature of single heterozygotes appeared indistinguishable from wild-type littermates (Fig. 7f–i). Collectively, these data indicate that VEGFR-3 may induce Notch target genes through FoxC2 independently of Notch ligand–receptor interactions (Fig. 7j).

DISCUSSION

Here we demonstrate that endothelial loss of VEGFR-3 leads to hypervascularization in developmental and tumour angiogenesis as well as in purely VEGF-driven angiogenesis. This finding contrasts with our previous data showing that VEGFR-3-blocking antibodies rather suppress angiogenesis[14,42]. Although seemingly in stark conflict, it is important to consider that the two phenotypes are a result of profoundly different perturbations of VEGFR-3. In the case of antibodies, the intracellular domain is free to interact with intracellular proteins, whereas the entire receptor is missing following genetic deletion.

Indeed, VEGFR-3 can be phosphorylated by the intracellular tyrosine kinase Src, activated downstream of integrins following cell adhesion to matrix collagen I, even in conditions in which VEGFR-3 tyrosine kinase activity is lost[33]. Here we showed that the tyrosine kinase domain of VEGFR-3 can be phosphorylated following endothelial cell adhesion to collagen I in the presence of specific antibodies that block ligand–receptor interactions. Given that endothelial cells adhere to collagen I during angiogenic invasion of tissues[43], it is likely that some phosphorylation of VEGFR-3 occurs also *in vivo* even in the presence of blocking antibodies or the absence of the ligand.

Our analysis of mice harbouring various allelic combinations of endothelial-cell-deleted (*i*Δ*EC*), kinase-dead mutant and wild-type *Vegfr3* allowed for a titration of both kinase activity and genetic dose of VEGFR-3. The combination of a 50% decrease in genetic dose and loss of kinase activity in the remaining allele (iΔEC/KD) represented a threshold for the degree of VEGFR-3 phosphorylation required for normal angiogenesis. Importantly, our previous results indicate that the kinase-dead mutant may exert dominant-negative activity[32], which is why it is likely not to precisely mimic the effect of VEGFR-3-blocking antibodies.

Our results indicate that VEGFR-3 controls Notch targets, but VEGFR-3 is also capable of inducing mitogenic signalling[14]. According to our model, the latter 'active' function is dependent on ligand binding and can be blocked by specific inhibitors, whereas the regulation of Notch can persist even in the presence of inhibitors (Fig. 7j). The elucidation of the ligand-independent, or 'passive', signalling modality may explain why compound

Nat Cell Biol. Author manuscript; available in PMC 2012 January 19.

– 156 –

deletion of both VEGFR-3 ligands, *Vegfc* and *Vegfd*, does not recapitulate the early embryonic lethality of *Vegfr3* gene-targeted mice[17], and why VEGFR-3-blocking antibodies, which prevent ligand-dependent activation of the receptor, suppress angiogenesis[14].

Interestingly, we observed a slight increase in the level of VEGFR-2 activity in cultured cells in which VEGFR-3 expression was silenced, whereas robust overexpression of wild-type, kinase-dead or ligand-binding-defective VEGFR-3 decreased the level of VEGFR-2 phosphorylation following VEGF stimulation[44]. Furthermore, we showed that VEGFR-2-blocking antibodies were able to rescue the hypervascularity resulting from endothelial deletion of *Vegfr3*, although morphologically the vessels remained abnormal. These findings indicate that VEGFR-3, although not capable of binding to VEGF, may act as a negative regulator of VEGF–VEGFR-2 signalling. Interestingly, implications towards such an interaction were already made in an elegant study demonstrating that VEGF can bring VEGFR-2 and VEGFR-3 to close proximity without inducing VEGFR-3 phosphorylation[45]. Importantly, we did not detect differences in the level of VEGFR-2 phosphorylation following VEGF stimulation in the presence of VEGFR-3-blocking antibodies.

The previous observations[45] place VEGFR-3 in VEGF–VEGFR-2 signalling clusters on the endothelial cell membrane and in subsequent signalosomes, which are known to contain multiple membrane-bound molecules that modulate the activity of VEGFRs, including ephrin-B2 (refs 46,47), claudin-like protein 24 (ref. 48), neuropilin-1 (ref. 49) and VE-cadherin[50]. It is therefore possible that VEGFR-3-blocking antibodies sterically disrupt the cluster or promote receptor internalization in addition to suppressing ligand-activated VEGFR-3 kinase activity. Conversely, loss of VEGFR-3 would allow its molecular partners to interact with VEGFR-2, which may modulate the signalling properties of this potent endothelial kinase.

We detected a significant decrease in the expression of multiple Notch target genes and the Notch ligand Dll4 in the *Vegfr3*[i4EC] retinas, and observed a rescue of the hypervascular phenotype following exogenous activation of the Notch signalling pathway. In contrast, VEGF-C was capable of inducing Notch target gene expression even in the presence of a potent Notch inhibitor, that is independently of the canonical Notch ligands, as well as potentiating the induction of Notch targets in response to Dll4–Notch interactions. Notch target gene induction stimulated by VEGF-C was suppressed by administration of a PI(3)K inhibitor, which has also been shown to suppress Notch target gene expression following stimulation with VEGF (refs 36,38) or cyclic adenosine monophosphate[37] (cAMP) in endothelial cells or endothelial cell progenitors, respectively.

We have previously established a genetic interaction for VEGFR-3 and FoxC2 in the regulation of lymphatic valve formation[40]. Previous studies have shown that FOXC2 directly regulates the expression of *DLL4* and *HEY2* (refs 38,41), possibly by interacting with the Notch intracellular domain[38] (NICD). Here we demonstrate that endothelial loss of *Vegfr3* leads to a pronounced downregulation of FoxC2, and *Foxc2*^{+/−};*Vegfr3*^{+/−} compound heterozygotes recapitulated the phenotype observed in *Vegfr3*[i4EC] homozygotes. Interestingly, *Notch1*^{+/−};*Vegfr3*^{+/−} compound heterozygous embryos exhibit increased lethality, whereas single heterozygotes survive in normal Mendelian ratios[51]. According to our findings and the published literature, it seems that VEGFR-3 can augment Notch signalling independently of canonical Notch ligand–receptor interactions through a mechanism involving FoxC2.

In zebrafish, VEGF-C controls angiogenesis before the formation of the lymphatic vascular system[52]. Interestingly, we detected induction of VEGF-C expression in macrophages at

sites of sprout fusion, and robust expression in cells localized at vessel branch points. Tie2-positive macrophages have been implicated in tumour angiogenesis[53] and as chaperones of sprout fusion during development[24], which is why it is of particular interest that the Tie2-positive macrophages were also VEGF-C positive. We observed similar vascular mispatterning, branching failure and a decreased level of Notch target gene expression in both *Vegfc* haploinsufficient mice and macrophage-deficient *op/op* mice. Although macrophages produce a plethora of growth factors[26], our studies implicate VEGF-C as a key factor in vascular branch formation on the basis of genetic loss-of-function experiments, as well as the spatiotemporally coincident expression of both VEGF-C and VEGFR-3 at sites of sprout fusion.

Importantly, the phenotype resulting from heterozygous loss of *Vegfc* is different from homozygous endothelial deletion of *Vegfr3*, as characterized by decreased and increased branching, respectively. Deficiency of the ligand is likely to lead to decreased levels of activity of both VEGFR-3 and VEGFR-2, and to affect the 'active' mode of VEGFR-3 signalling, which promotes angiogenesis, whereas the passive mode of signalling is still able to function through intracellular activation of VEGFR-3. However, the loss of *Vegfr3* abolishes both signalling modalities, leading to a significant decrease in the level of Notch signalling. Unlike the loss of VEGF-C, which resulted in reduced angiogenesis, the loss of VEGFR-3 did not negatively affect VEGFR-2 signalling; rather a small increase was observed.

VEGFR-3 signals seem to have an important role in a mechanism for the rapid conversion of tip cells to stalk cells, which is required at points of sprout fusion, where tip cells of opposing sprouts meet and establish cell–cell junctions. Our data support a model in which VEGF-C-producing macrophages stimulate VEGFR-3-positive tip cells to turn on Notch target genes, which leads to decreased sensitivity to VEGF and downregulation of VEGFR-3 in these cells[14,27,28], facilitating the assembly of vascular loops. In support of this model, we observed FoxC2 expression only in stalk cells and in endothelial cells forming vascular loops, but not in tip cells. Interestingly, *Vegfc* expression is also found in angiogenic endothelial cells during development[14], indicating the possibility of autocrine VEGF-C–VEGFR-3 interactions that may produce qualitatively distinct signals.

Our data indicate that BECs are instructed to migrate and proliferate primarily by VEGFR-2, whereas VEGFR-3 is the primary receptor driving differentiation signals towards the stalk-cell phenotype by activating Notch target gene expression through FoxC2. However, when VEGFR-2 is blocked, VEGFR-3 kinase activity can partially compensate for the loss of VEGFR-2 activity in driving the growth of endothelial cells, and vice versa[14]. Indeed, we have previously shown that VEGFR-3 activation can promote proliferation of BECs *in vivo*, but these signals are weak when compared with those originating from VEGFR-2 (refs 14,54). However, blocking VEGFR-3 augmented the effect of VEGF–VEGFR-2 axis inhibitors by providing additional inhibition of angiogenesis[14], which reflects the capacity of VEGFR-3 for angiogenic signalling.

Our results using inducible gene targeting elucidate a bimodal function for VEGFR-3 in angiogenesis as a driver of both growth and differentiation of endothelial cells, which could not have been discovered by studying specific inhibitors alone, attesting to the power of mouse molecular genetics. VEGFR-3-blocking antibodies and kinase inhibitors are capable of targeting only the 'active' arm of VEGFR-3 signalling, whereas the 'passive' arm could be eliminated only by genetic deletion of the receptor (Fig. 7j). Our results support an intricate mechanism that controls the formation and integrity of vascular micro-anastomoses during angiogenesis, and reinforce the concept of augmentation of Notch signals by receptor

tyrosine kinase activation, which may provide additional tools for the therapeutic manipulation of the blood vascular system.

METHODS

Methods and any associated references are available in the online version of the paper at http://www.nature.com/naturecellbiology

Supplementary Material

Refer to Web version on PubMed Central for supplementary material.

Acknowledgments

References

1. Ferrara N, et al. Heterozygous embryonic lethality induced by targeted inactivation of the VEGF gene. Nature. 1996; 380:438–442.

2. Carmeliet P, et al. Abnormal blood vessel development and lethality in embryos lacking a single VEGF allele. Nature. 1996; 380:435–439. [PubMed: 8602241]

3. Shalaby F, et al. Failure of blood island formation and vasculogenesis in Flk-1-deficient mice. Nature. 1995; 376:62–66. [PubMed: 7596435]

4. Gille H, et al. Analysis of biological effects and signaling properties of Flt-1 (VEGFR-1) and KDR (VEGFR-2). A reassessment using novel receptor-specific vascular endothelial growth factor mutants. J Biol Chem. 2001; 276:3222–3230. [PubMed: 11058584]

5. Tammela T, Alitalo K. Lymphangiogenesis: molecular mechanisms and future promise. Cell. 2010; 140:460–476. [PubMed: 20178740]

6. Dixelius J, et al. Ligand-induced vascular endothelial growth factor receptor-3 (VEGFR-3) heterodimerization with VEGFR-2 in primary lymphatic endothelial cells regulates tyrosine phosphorylation sites. J Biol Chem. 2003; 278:40973–40979. [PubMed: 12881528]

7. Nilsson I, et al. VEGF receptor 2/3 heterodimers detected *in situ* by proximity ligation on angiogenic sprouts. EMBO J. 2010; 29:1377–1388. [PubMed: 20224550]

8. Dumont DJ, et al. Cardiovascular failure in mouse embryos deficient in VEGF receptor-3. Science. 1998; 282:946–949. [PubMed: 9794766]

Nat Cell Biol. Author manuscript; available in PMC 2012 January 19.

– 159 –

9. Covassin LD, Villefranc JA, Kacergis MC, Weinstein BM, Lawson ND. Distinct genetic interactions between multiple Vegf receptors are required for development of different blood vessel types in zebrafish. Proc Natl Acad Sci USA. 2006; 103:6554–6559. [PubMed: 16617120]

10. Kaipainen A, et al. Expression of the *fms*-like tyrosine kinase FLT4 gene becomes restricted to lymphatic endothelium during development. Proc Natl Acad Sci USA. 1995; 92:3566–3570. [PubMed: 7724599]

11. Lohela M, Helotera H, Haiko P, Dumont DJ, Alitalo K. Transgenic induction of vascular endothelial growth factor-C is strongly angiogenic in mouse embryos but leads to persistent lymphatic hyperplasia in adult tissues. Am J Pathol. 2008; 173:1891–1901. [PubMed: 18988807]

12. Paavonen K, Puolakkainen P, Jussila L, Jahkola T, Alitalo K. Vascular endothelial growth factor receptor-3 in lymphangiogenesis in wound healing. Am J Pathol. 2000; 156:1499–1504. [PubMed: 10793061]

13. Valtola R, et al. VEGFR-3 and its ligand VEGF-C are associated with angiogenesis in breast cancer. Am J Pathol. 1999; 154:1381–1390. [PubMed: 10329591]

14. Tammela T, et al. Blocking VEGFR-3 suppresses angiogenic sprouting and vascular network formation. Nature. 2008; 454:656–660. [PubMed: 18594512]

15. Karkkainen MJ, et al. Vascular endothelial growth factor C is required for sprouting of the first lymphatic vessels from embryonic veins. Nat Immunol. 2004; 5:74–80. [PubMed: 14634646]

16. Baldwin ME, et al. Vascular endothelial growth factor D is dispensable for development of the lymphatic system. Mol Cell Biol. 2005; 25:2441–2449. [PubMed: 15743836]

17. Haiko P, et al. Deletion of vascular endothelial growth factor C (VEGF-C) and VEGF-D is not equivalent to VEGF receptor 3 deletion in mouse embryos. Mol Cell Biol. 2008; 28:4843–4850. [PubMed: 18519586]

18. Gerhardt H, et al. VEGF guides angiogenic sprouting utilizing endothelial tip cell filopodia. J Cell Biol. 2003; 161:1163–1177. [PubMed: 12810700]

19. Hellstrom M, et al. Dll4 signalling through Notch1 regulates formation of tip cells during angiogenesis. Nature. 2007; 445:776–780. [PubMed: 17259973]

20. Suchting S, et al. The Notch ligand Delta-like 4 negatively regulates endothelial tip cell formation and vessel branching. Proc Natl Acad Sci USA. 2007; 104:3225–3230. [PubMed: 17296941]

21. Roca C, Adams RH. Regulation of vascular morphogenesis by Notch signaling. Genes Dev. 2007; 21:2511–2524. [PubMed: 17938237]

22. Kamei M, et al. Endothelial tubes assemble from intracellular vacuoles *in vivo*. Nature. 2006; 442:453–456. [PubMed: 16799567]

23. Strilic B, et al. The molecular basis of vascular lumen formation in the developing mouse aorta. Dev Cell. 2009; 17:505–515. [PubMed: 19853564]

24. Fantin A, et al. Tissue macrophages act as cellular chaperones for vascular anastomosis downstream of VEGF-mediated endothelial tip cell induction. Blood. 2010; 116:829–840. [PubMed: 20404134]

25. Kubota Y, et al. M-CSF inhibition selectively targets pathological angiogenesis and lymphangiogenesis. J Exp Med. 2009; 206:1089–1102. [PubMed: 19398755]

26. Qian BZ, Pollard JW. Macrophage diversity enhances tumor progression and metastasis. Cell. 2010; 141:39–51. [PubMed: 20371344]

27. Siekmann AF, Lawson ND. Notch signalling limits angiogenic cell behaviour in developing zebrafish arteries. Nature. 2007; 445:781–784. [PubMed: 17259972]

28. Benedito R, et al. The notch ligands Dll4 and Jagged1 have opposing effects on angiogenesis. Cell. 2009; 137:1124–1135. [PubMed: 19524514]

29. Claxton S, et al. Efficient, inducible Cre-recombinase activation in vascular endothelium. Genesis. 2008; 46:74–80. [PubMed: 18257043]

30. Le Bras B, et al. VEGF-C is a trophic factor for neural progenitors in the vertebrate embryonic brain. Nat Neurosci. 2006; 9:340–348. [PubMed: 16462734]

31. Skobe M, et al. Concurrent induction of lymphangiogenesis, angiogenesis, and macrophage recruitment by vascular endothelial growth factor-C in melanoma. Am J Pathol. 2001; 159:893–903. [PubMed: 11549582]